[CANCER RESEARCH 57, 1664–1667, May 1, 1997]

Advances in Brief

Genetic Interactions between *atm* and *p53* Influence Cellular Proliferation and Irradiation-induced Cell Cycle Checkpoints[1]

Christoph Heiner Westphal, Cornelius Schmaltz, Sheldon Rowan, Ari Elson, David Erich Fisher, and Philip Leder[2]

Department of Genetics and Howard Hughes Medical Institute, Harvard Medical School [C. H. W., P. L.], and Department of Pediatric Oncology, Dana-Farber Cancer Institute and Harvard Medical School [C. S., S. R., D. E. F.], and Department of Molecular Genetics, The Weizmann Institute of Science, Rehovot 76100 Israel [A. E.]

Abstract

Ataxia-telangiectasia and Li-Fraumeni syndrome, pleiotropic disorders caused by mutations in the genes *atm* and *p53*, share a marked increase in cancer rates. A number of studies have argued for an interaction between these two genes (for comprehensive reviews, see M. S. Meyn, Cancer Res., 55: 5991–6001, 1995, and M. F. Lavin and Y. Shiloh, Annu. Rev., Immunol., *15*: 177–202, 1996). Specifically, *atm* is placed upstream of *p53* in mediating G_1-S cell cycle checkpoint control, and both *atm* and *p53* are believed to influence cellular proliferation. To analyze the genetic interactions of *atm* and *p53*, mouse embryonic fibroblasts (MEFs) homozygously deficient for both *atm* and *p53* were used to assess cell cycle and growth control. These double-null fibroblasts proliferate rapidly and fail to exhibit the premature growth arrest seen with *atm*-null MEFs. MEFs null for both *atm* and *p53* do not express any $p21^{cipl/wafl}$, showing that *p53* is required for $p21^{cipl/wafl}$ expression in an *atm*-null background. By contrast, homozygous loss of either *atm*, *p53*, or both results in similar abnormalities of the irradiation-induced G_1-S cell cycle checkpoint. Our results suggest two separate pathways of interaction between *atm* and *p53*, one linear, involving G_1-S cell cycle control, and another more complex, involving aspects of growth regulation.

Introduction

Ataxia-telangiectasia is a multifaceted disorder marked by progressive neurological degeneration, specific immunodeficiencies, telangiectasias, lymphoreticular malignancies, infertility, growth retardation, and premature signs of aging. Recently, three laboratories have reported the generation of mice null for *atm* (1–3). These mice are small and prone to thymic lymphomas and yield MEFs[3] that undergo growth arrest rapidly. Mice deficient in *p53* are similarly prone to cancers, which are also predominantly thymic lymphomas (4, 5). *atm* and *p53* are believed to interact in mediating DNA damage-associated cell cycle checkpoints and apoptosis, and both genes have been implicated in regulating cellular proliferation (6, 7). To analyze genetic interactions between *atm* and *p53*, MEFs were derived from mice bearing homozygous null mutations in *atm*, in *p53*, or in both genes. The predisposition to cell growth arrest and the fidelity of the irradiation-induced G_1-S cell cycle checkpoint were analyzed in cell lines null for both genes. We find that the additional loss of *p53* rescues the growth arrest phenotype seen in *atm*-null MEFs. In addition, homozygous loss of *atm*, *p53*, or both *atm* and *p53* abrogates the ionizing radiation-induced G_1-S checkpoint. These results argue for a role for *p53* in mediating the growth arrest observed in the *atm*-null background and provide a description of the genetic interactions between the *p53* and *atm* genes in a linear pathway regulating cell cycle control.

Materials and Methods

Derivation of MEFs. MEFs were derived using standard procedures (8). Day 11.5 to 16.5 post coitum embryos were dissociated, treated with DNase and trypsin, and plated in DMEM containing 15% FCS. DNA for Southern analysis was extracted from embryo heads.

Growth Assays and Passaging Experiments. MEF growth was assessed as described previously (1). Four $\times$ 10^4 cells (all at first passage) obtained from tissue culture dishes of equivalent density were plated in duplicate wells on six-well tissue culture plates. Cells were trypsinized and counted in duplicate using a hemocytometer at days 2, 4, 6, and 8 after plating. Each data point represents the average of duplicate wells.

Cell lines homozygously deficient in *atm*, *p53*, or both were passaged continuously using 1:5 dilutions in tissue culture until growth arrest was observed. The *atm*-null cell lines underwent growth arrest between passages 3 and 4, whereas the *p53* and *atm/p53* doubly deficient cell lines continued at a doubling rate of 18–20 h past passage 20.

Irradiation and Fluorescence-activated Cell Sorting Analysis. Unsynchronized early-passage (p2–p4) MEFs, growing on tissue culture dishes, were irradiated from a ^{137}Cs-source (Gammacell 40, Atomic Energy of Canada, Ltd.) at a dose rate of 1 Gy/min. Cells were harvested 16 h after irradiation, fixed in 50% ethanol, and stained for 30 min in a solution of 2.5 μg/ml propidium iodide and 50 μg/ml RNase A. Flow cytometry was carried out on a FACScan (Becton Dickinson) using CellQuest Software. The data were analyzed subsequently with ModFitLT V1.01 for cell cycle determination.

Protein Analysis. Early-passage wild-type, *atm*-null, *p53*-null, and double-null cells were harvested, and 500,000 cells were lysed to make extracts. Entire extracts were separated by 13% PAGE and transferred onto a nitrocellulose filter (Schleicher & Schuell). Protein was detected using a polyclonal $p21^{cipl/wafl}$ antibody (C-19; Santa Cruz Biotechnology) or a β-tubulin-specific antibody (TUB 2.1, Sigma Chemical Co.) Filters were incubated with horseradish peroxidase-coupled secondary antibody (Cappel) and visualized with enhanced chemiluminescence.

Results

Generation of *atm*(−/−) p53(−/−) MEFs. To produce MEFs null for both the *atm* and *p53* genes, compound heterozygotic [*atm*(+/−) *p53*(+/−)] mice were mated, and pregnant females were sacrificed to derive MEFs between 11.5 and 16.5 days post coitum. A total of 79 primary cell lines were derived in this manner, yielding all possible genotypic combinations, including two deficient for both *atm* and *p53*. These cell lines were used for subsequent growth experiments and cell cycle analysis.

Control of Cellular Proliferation Is Mediated by *atm* and *p53*. The effects of *atm* and *p53* on cellular proliferation were studied via cell growth experiments on early-passage MEFs. As shown in Fig. 1*A*, and consistent with earlier observations, *atm*-null MEFs undergo fewer than four doublings before undergoing growth arrest (1–3). By contrast, homozygous deletion of *p53* in an *atm*-null background

Received 2/26/97; accepted 3/24/97.

The costs of publication of this article were defrayed in part by the payment of page charges. This article must therefore be hereby marked *advertisement* in accordance with 18 U.S.C. Section 1734 solely to indicate this fact.

[1] This work was supported by the Howard Hughes Medical Institute (to P. L.) and by NIH Grants CA69531 and AR43369 (to D. E. F.). D. E. F. is a Pew Foundation scholar and a scholar of the James S. McDonnall Foundation. C. H. W. is a Sandoz Fellow. C. S. is the recipient of a scholarship from the Deutsche Forschungsgemeinschaft. S. R. is supported by a predoctoral fellowship from the Howard Hughes Medical Institute. A. E. is an Alon Fellow and the incumbent of the Adolfo and Evelyn Blum Chair.

[2] To whom requests for reprints should be addressed, at Department of Genetics, Harvard Medical School, 200 Longwood Avenue, Boston, MA 02115.

[3] The abbreviation used is: MEF, mouse embryonic fibroblast.

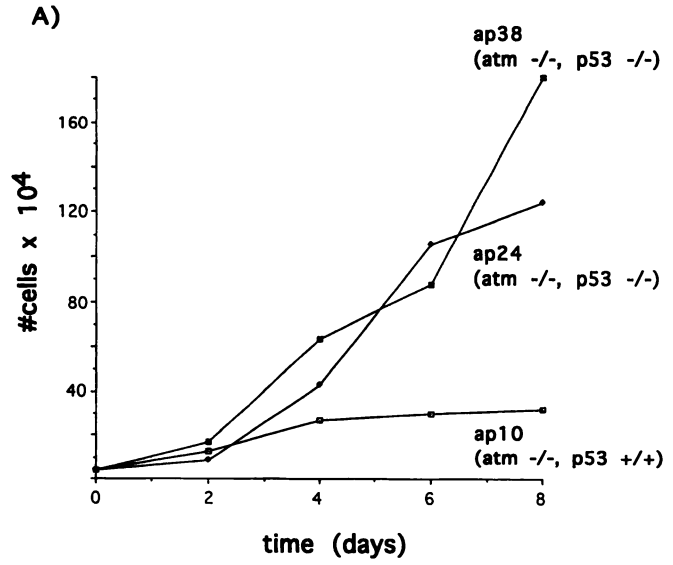

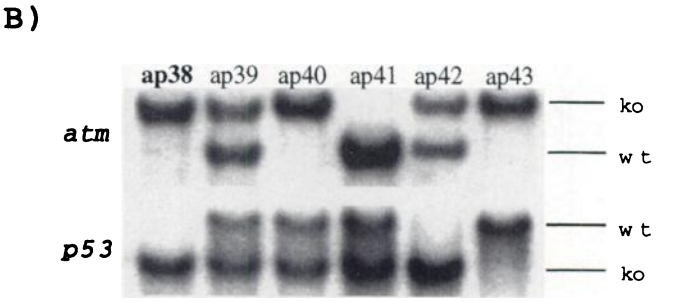

Fig. 1. *A*, MEFs deficient in both *atm* and *p53* proliferate more rapidly than MEFs deficient in *atm* alone. Both double-null lines grow significantly faster than any *atm*-deficient cell line described to date. *B*, Southern blot analysis of representative MEFs derived in the present cross. The *atm* knockout allele is 7 kb, and the wild-type allele is 5 kb (2). The *p53* knockout allele is 8 kb, and the wild-type allele is 16 kb (5). MEF primary cell line ap38 (*bold*), the growth properties of which are described in *A*, is *atm*(−/−) *p53*(−/−). MEFs ap39 to ap43 represent a range of other genotypic combinations. *ko*, knockout allele; *wt*, wild-type allele.

overcomes this growth arrest (two independently derived MEFs, ap38 and ap24, are depicted in Fig. 1*A*). The signal for growth arrest seen in *atm*-null MEFs is hence dependent on *p53* function. Fig. 1*B* shows a representative Southern blot of MEFs derived in the present cross, including ap38, one of the double-null MEFs used for the growth experiments shown in Fig. 1*A*. *atm*(−/−) *p53*(−/−) cells have been monitored for more than 20 passages without signs of the slowed growth indicative of crisis (data not shown). *atm*(+/+) *p53*(−/−) cells were monitored in parallel and proliferated at the same rate over 20 passages.

To address the role of $p21^{cipl/wafl}$ in the control of cellular proliferation, protein expression was analyzed in wild-type, single-null, and double-null cells. $p21^{cipl/wafl}$ protein is present at equivalent levels in both proliferating and nonproliferating *atm*-null MEFs and is expressed at lower levels in wild-type cells (Fig. 2, *Lanes 1, 2,* and *5*; see also Ref. 3). Interestingly, neither *atm*(−/−) *p53*(−/−) nor *atm*(+/+)*p53*(−/−) cells express $p21^{cipl/wafl}$, as measured by Western blot (Fig. 2, *Lanes 3* and *4*, respectively). These observations support the view that *p53* is the dominant modulator of $p21^{cipl/wafl}$ expression, whereas loss of *atm* leads to up-regulation of $p21^{cipl/wafl}$ protein levels via direct or indirect mechanisms (see also Fig. 4*A*).

***atm*(−/−) *p53*(−/−) MEFs Have an Impaired Irradiation-induced G_1-S Cell Cycle Checkpoint.** Patients with ataxia-telangiectasia and Li-Fraumeni syndrome are known to develop cancers at an increased rate. In both cases, the pathogenic role of increased genomic fragility has been implicated (9, 10). Deficiencies in either *atm* or *p53* lead to profound defects in γ-irradiation-induced cell cycle checkpoints, which likely play a role in the predisposition to cancer seen in both diseases (11). *p53* activation of $p21^{cipl/wafl}$ plays a central role in the G_1-S checkpoint after certain types of DNA damage, such as that caused by ionizing radiation (8, 12). The G_2-M damage-activated checkpoint, on the other hand, appears to be partially *p53* independent (13). Loss of *atm* has a complex effect on the G_2-M cell cycle checkpoint (14–17), which is felt to be independent of *p53*. A more detailed analysis of the G_2-M checkpoint is hence not presented here.

To understand the epistatic relationship between *atm* and *p53* in cell cycle control, *atm/p53* double-null cells were compared to littermate control MEFs with respect to the function of their G_1-S cell cycle checkpoint in response to γ irradiation. The primary data are presented in Fig. 3, *A–D*. Because *atm* homozygously deficient cell lines undergo growth arrest quite rapidly, Southern analysis of embryos was completed within 2.5 days after harvesting, and *atm*-null cells were subjected immediately to cell cycle analysis. The cell cycle analysis involved γ-irradiating cells at the indicated doses and harvesting cells 16 h later for fixation, staining, and analysis by flow cytometry.

As shown in Fig. 3*A*, wild-type cells show a functional checkpoint at G_1-S. By contrast, the G_1-S checkpoint is impaired significantly in *p53*-null cells (Fig. 3*B*). Similarly, in the case of the *atm*-null MEFs (Fig. 3*C*), there is a clear deficiency in the G_1-S checkpoint, which is likely underestimated because a significant proportion of these cells are already growth arrested and residing in G_0. This premature growth arrest has been documented extensively (1–3). Cells null in both *atm* and *p53* again show loss of the G_1-S checkpoint (Fig. 3*D*).

Fig. 3*E* represents the percentage change seen in G_1-G_0 after 5 or 10 Gy of irradiation. These data are consistent at 5, 10, and 20 Gy, showing that wild-type MEFs manifest an increasing percentage of cells in G_1-G_0 after irradiation, whereas single-and double-null cells show a decreasing percentage over the range of doses analyzed. Note that both double-null MEFs derived in this cross are shown here, and that the percentage decrease in G_1-G_0 is similar in these two primary lines. The results presented in Fig. 3*A–E* support a previously proposed model in which *atm* and *p53* assume equivalent roles in mediating irradiation-induced G_1-S cell cycle arrest, consistent with their participation in a linear regulatory pathway (Fig. 4*B*; Refs. 14 and 15).

Discussion

Loss of *p53* Suppresses the Growth Arrest Seen in *atm*-null MEFs. All previously described human and mouse *atm*-deficient fibroblast cell lines show significant growth defects. In the mouse, the growth

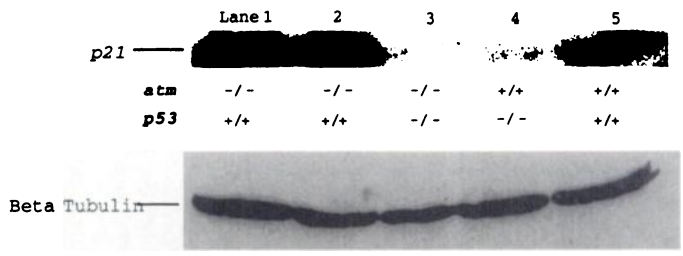

Fig. 2. $p21^{cipl/wafl}$ protein can be visualized in an *atm*-null, but not in *p53*-null or *atm/p53*-double-null MEFs. $p21^{cipl/wafl}$ is expressed at high levels in both proliferating (*Lane 1*) and nonproliferating (*Lane 2*) *atm* homozygously deficient cells. $p21^{cipl/wafl}$ is completely absent in *p53*-null and double-null MEFs (*Lanes 3* and *4*, respectively). $p21^{cipl/wafl}$ is present in wild-type MEFs but is reduced in comparison to *atm*-null MEFs (*Lane 5*). A β-tubulin loading control is shown. *p53* levels are essentially undetectable in each of these cell lines, in agreement with previous results (Ref. 3; data not shown) indicating that *p53* is only induced after irradiation in MEFs.

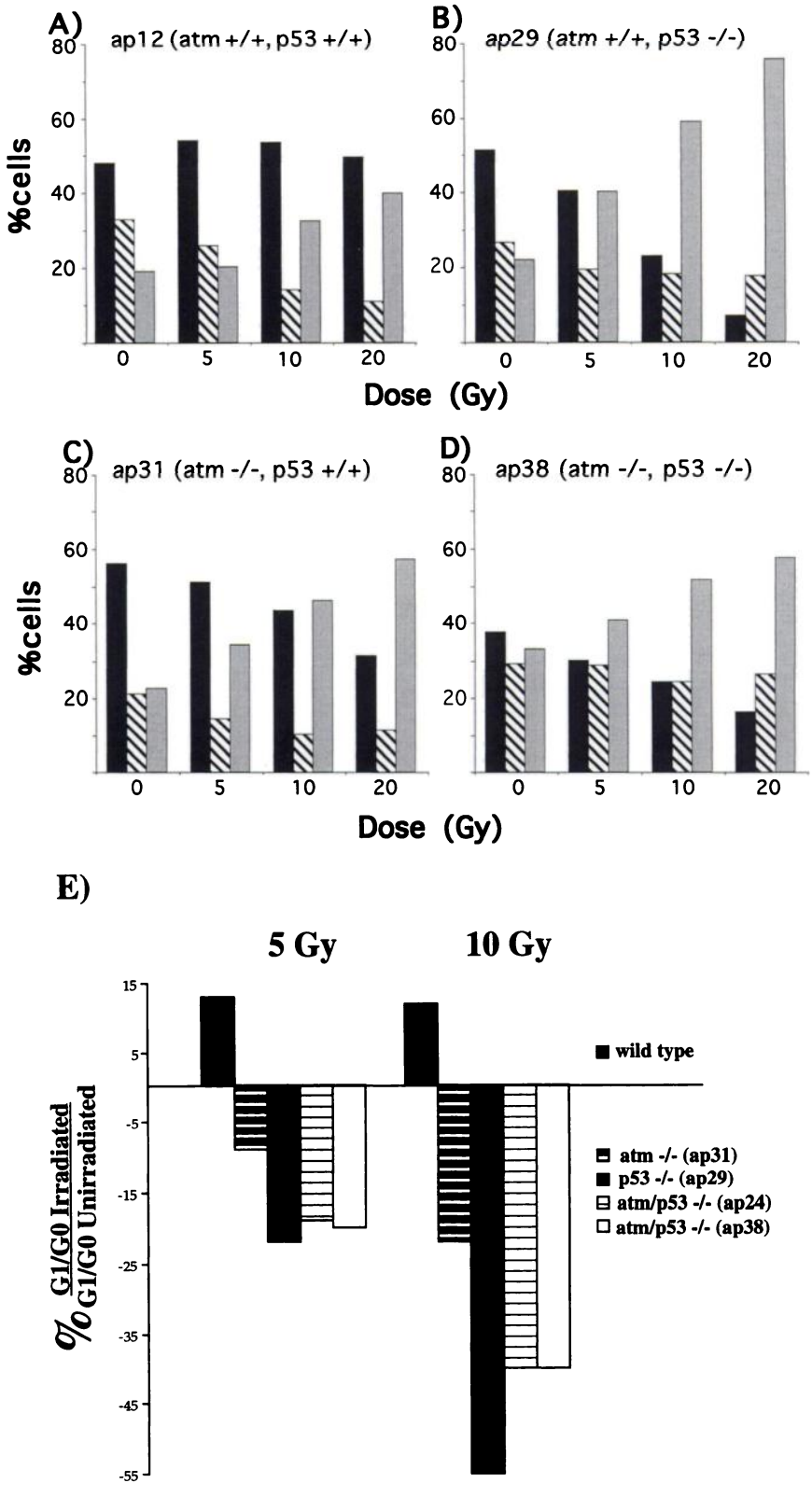

Fig. 3. MEFs deficient in both *atm* and *p53* show lack of the G_1-S checkpoint. *A*, intact G_1-S checkpoint in an *atm*(+/+) *p53*(+/+) control cell line. *B* and *C* show lack of the G_1-S checkpoint in *atm*(+/+) *p53*(−/−) and *atm*(−/−) p53(+/+) control cell lines, respectively. *D*, a representation of the cell cycle profile of *atm*(−/−) *p53*(−/−) cells, again with deficiency in the G_1-S cell cycle checkpoint. *E* represents a direct comparison of the percentage change in G_1-G_0 after 5 and 10 Gy of irradiation (compared to unirradiated) in two double-null cell lines, one wild-type cell line and each single-null cell line. These data are based on the primary data presented in *A–D*. Note that the percentage decrease in G_1-G_0 phase seen in *atm*(−/−) *p53*(+/+) is less pronounced than that seen in *atm*(+/+) *p53*(−/−) and *atm*(−/−) *p53*(−/−) cells. This is likely due to an increase in G_0 phase of these cells, because these cells are about to undergo growth arrest, as described here and previously (1–3). A qualitative difference can be seen between wild-type (with increased G_1-G_0 phase after irradiation), and single- and double-null cells (with decreased G_1-G_0 phase after irradiation). This difference was reproducible over the range of doses shown in *A–D*, with each of these observations representing an independent experimental observation. Finally, both double-null cell lines represented in *E* showed virtually identical percentage decreases in G_1-G_0 at all irradiation doses. Phases: ■, G_1-G_0; ▧, S; and □, G_2.

arrest is especially severe, leading to a senescent appearance at the third passage in tissue culture (1–3). In contrast, deletion of either $p21^{cipl/wafl}$ or *p53* increases MEF proliferative rates (8). Here we have shown that the homozygous genetic deletion of *p53* in an *atm*-deficient background overcomes the growth arrest seen in *atm*-null MEFs.

These results argue for a dominant role for *p53* in mediating MEF growth arrest, because MEFs null for *atm* and *p53* proliferate much more rapidly than MEFs deficient in *atm* alone. These double-null cells grow as rapidly as cells null for *p53*. Although the exact role, if any, of $p21^{cipl/wafl}$ is presently not clear, it is possible that a portion of the growth arrest seen in *atm*-null cells is mediated by a $p21^{cipl/wafl}$-dependent mechanism, because $p21^{cipl/wafl}$ is overexpressed in *atm*-null cells. These elements can be brought together in the simplified model outlined in Fig. 4*A*. It is important to note that suppression of

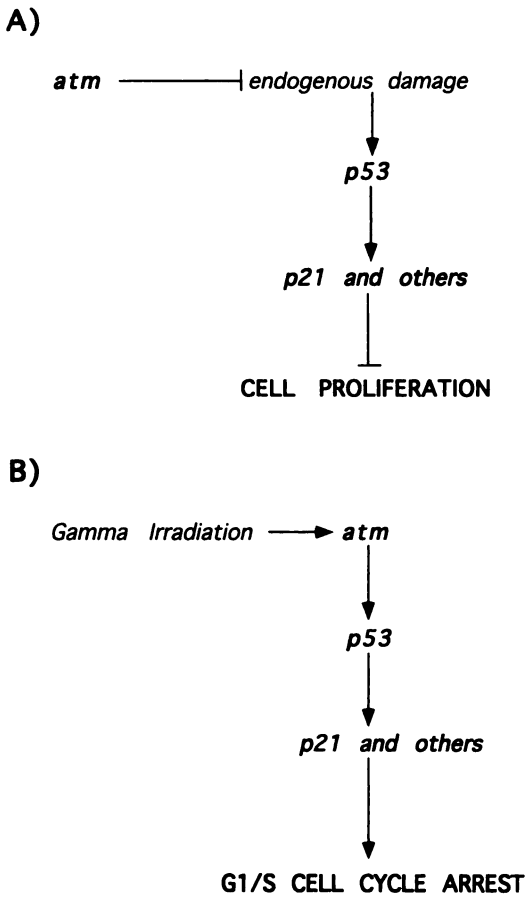

Fig. 4. Diagrammatic representation of the putative actions of *atm* and *p53* as they affect MEF cellular proliferation and the G_1-S cell cycle checkpoint. These diagrams are based on previous models (6, 7, 14, 15, 18) and the observations described in this study. *A* indicates that loss of *atm* leads to the sensing and/or production of endogenous cellular damage (2), signaling MEF growth arrest via *p53* and p21. Note that signals through *p53* and p21 may be direct or indirect. Here, homozygous loss of *atm* leads to growth arrest, whereas homozygous loss of *p53* or both *atm* and *p53* leads to relief of inhibition and rapid cellular proliferation. *B* shows that γ-irradiation induces a G_1-S cell cycle arrest directly via *atm* and *p53*. In this case, homozygous loss of either *atm*, *p53*, or both results in similar defects in the G_1-S cell cycle checkpoint.

the *atm*-null growth arrest by genetic deletion of *p53* could also be consistent with a parallel or downstream effect of *p53*.

***atm* and *p53* Show Equivalent Effects in Facilitating Irradiation-induced Cell Cycle Checkpoints.** Because cells deficient in either *atm* or *p53* are defective in the radiation-induced G_1-S cell cycle checkpoint, it is possible to imagine that they act along the same or parallel pathways to induce this checkpoint. If the pathways were parallel, the collective effects of both pathways might be additive and their mutual loss would lead to a more severe loss of checkpoint control. To begin to distinguish between these possibilities, we have assessed radiation-induced checkpoint control in MEFs homozygously deficient for either *p53* or *atm* and have compared their response to MEFs homozygously deficient in both *atm* and *p53*. Homozygous loss of either gene clearly impairs the irradiation-induced G_1-S checkpoint, whereas deletion of both genes in tandem does not appear to significantly exacerbate this phenotype. These and previous observations argue for an equivalent role for *atm* and *p53* in a common pathway mediating the irradiation-induced G_1-S checkpoint (Fig. 4*B*; Refs. 14 and 15).

Interestingly, loss of $p21^{cipl/wafl}$ similarly perturbs the G_1-S checkpoint (8, 12). Moreover, $p21^{cipl/wafl}$-null mice do not appear to develop cancer at increased frequencies (8). Inasmuch as loss of either *atm* or *p53* predisposes to malignancy in both mouse and human, this phenotype seems less likely to involve a $p21^{cipl/wafl}$-mediated signal transduction pathway. The studies reported here highlight the paradox that *atm* function may be either growth-inhibiting (at the G_1-S radiation-induced cell cycle checkpoint) or growth-promoting (in MEFs grown *in vitro*), and that *p53* may modulate both of these effects.

References

1. Barlow, C., Hirotsune, S., Paylor, R., Liyanage, M., Eckhaus, M., Collins, F., Shiloh, Y., Crawley, J. N., Ried, T., Tagle, D., and Wynshaw-Boris, A. atm-deficient mice: a paradigm of ataxia telangiectasia. Cell, *86:* 159–171, 1996.
2. Elson, A., Wang, Y., Daugherty, C. J., Morton, C. C., Zhou, F., Campos-Torres, J., and Leder, P. Pleiotropic defects in ataxia-telangiectasia protein-deficient mice. Proc. Natl. Acad. Sci. USA, *93:* 13084–13089, 1996.
3. Xu, Y., and Baltimore, D. Dual roles of ATM in the cellular response to radiation and in cell growth control. Genes Dev., *10:* 2401–2410, 1996.
4. Jacks, T., Remington, L., Williams, B. O., Schmitt, E. M., Halachmi, S., Bronson, R. T., and Weinberg, R. A. Tumor spectrum analysis in p53-mutant mice, Curr. Biol., *4:* 1–7, 1994.
5. Donehower, L. A., Harvey, M., Slagle, B. L., McArthur, M. J., Montgomery, C. A., Jr., Butel, J. S., and Bradley, A. Mice deficient for p53 are developmentally normal but susceptible to spontaneous tumours. Nature (Lond.), *356:* 215–221, 1992.
6. Enoch, T., and Norbury, C. Cellular responses to DNA damage: cell-cycle checkpoints, apoptosis and the roles of p53 and ATM, Trends Biochem. Sci., *20:* 426–430, 1995.
7. Hawley, R. S., and Friend, S. H. Strange bedfellows in even stranger places: the role of ATM in meiotic cells, lymphocytes, tumors, and its functional links to p53, Genes Dev. , *10:* 2383–2388, 1996.
8. Deng, C., Zhang, P., Harper, J. W., Elledge, S. J., and Leder, P. Mice lacking p21CIP1/WAF1 undergo normal development, but are defective in G1 checkpoint control. Cell, *82:* 675–684, 1995.
9. Meyn, M. S. High spontaneous intrachromosomal recombination rates in ataxia-telangiectasia. Science (Washington DC), *260:* 1327–1330, 1993.
10. Meyn, M. S., Strasfeld, L., and Allen, C. Testing the role of p53 in the expression of genetic instability and apoptosis in ataxia-telangiectasia. Int. J. Radiat. Biol., *66:* S141–S149, 1994.
11. Canman, C. E., Wolff, A. C., Chen, C. Y., Fornace, A. J., Jr., and Kastan, M. B. The p53-dependent G_1 cell cycle checkpoint pathway and ataxia-telangiectasia. Cancer Res., *54:* 5054–5058, 1994.
12. Brugarolas, J., Chandrasekaran, C., Gordon, J. I., Beach, D., Jacks, T., and Hannon, G. J. Radiation-induced cell cycle arrest compromised by p21 deficiency, Nature (Lond.), *377:* 552–557, 1995.
13. Jacks, T., and Weinberg, R. A. Cell-cycle control and its watchman. Nature (Lond.), *381:* 643–644, 1996.
14. Meyn, M. S. Ataxia-telangiectasia and cellular responses to DNA damage. Cancer Res., *55:* 5991–6001, 1995.
15. Lavin, M. F. and Shiloh, Y. The genetic defect in ataxia-telangiectasia, Annu. Rev. Immunol., *15:* 177–202, 1996.
16. Beamish, H., and Lavin, M. F. Radiosensitivity in ataxia-telangiectasia: anomalies in radiation-induced cell cycle delay. Int. J. Radiat. Biol., *60:* 791–802, 1994.
17. Thacker, J. Cellular radiosensitivity in ataxia-telangiectasia. Int. J. Radiat. Biol., *66:* S87–S96, 1994.
18. Kastan, M. B., Zhan, Q., el-Deiry, W. S., Carrier, F., Jacks, T., Walsh, W. V., Plunkett, B. S., Vogelstein, B., and Fornace, A. J., Jr. A mammalian cell cycle checkpoint pathway utilizing p53 and GADD45 is defective in ataxia-telangiectasia. Cell, *71:* 587–597, 1992.

Genetic Interactions between *atm* and *p53* Influence Cellular Proliferation and Irradiation-induced Cell Cycle Checkpoints

Christoph Heiner Westphal, Cornelius Schmaltz, Sheldon Rowan, et al.

Cancer Res 1997;57:1664-1667.